Advances in Rheumatology

RESEARCH

Open Access

Screening crucial lncRNAs and genes in osteoarthritis by integrated analysis

Jun Wang, Yumin Zhang, Tao Ma, Tao Wang, Pengfei Wen, Wei Song* and Binfei Zhang*

Abstract

Background Osteoarthritis (OA) is one of the most frequent chronic diseases with high morbidity worldwide, marked by degradation of the cartilage and bone, joint instability, stiffness, joint space stenosis and subchondral sclerosis. Due to the elusive mechanism of osteoarthritis (OA), we aimed to identify potential markers for OA and explore the molecular mechanisms underlying OA.

Methods Expression profiles data of OA were collected from the Gene Expression Omnibus database to identify differentially expressed mRNAs (DEmRNAs) and differentially expressed lncRNAs (DElncRNAs) in OA. Functional annotation and protein–protein interaction (PPI) networks were performed. Then, nearby DEmRNAs of DElncRNAs was obtained. Moreover, GO and KEGG pathway enrichment analysis of nearby DEmRNAs of DElncRNAs was performed. Finally, expression validation of selected mRNAs and lncRNAs was performed by quantitative reverse transcriptase-polymerase chain reaction.

Results In total, 2080 DEmRNAs and 664 DElncRNAs were determined in OA. PI3K-Akt signaling pathway, Endocytosis and Rap1 signaling pathway were significantly enriched KEGG pathways in OA. YWHAB, HSPA8, NEDD4L and SH3KBP1 were four hub proteins in PPI network. The AC093484.4/TRPV2 interact pair may be involved in the occurrence and development of OA.

Conclusion Our study identified several DEmRNAs and DElncRNAs associated with OA. The molecular characters could provide more information for further study on OA.

Keywords Osteoarthritis, GEO, lncRNA, mRNA, Bioinformatics, Diagnosis

Background

Osteoarthritis (OA) is one of the most frequent chronic diseases with high morbidity worldwide, marked by degradation of the cartilage and bone, joint instability, stiffness, joint space stenosis and subchondral sclerosis [1]. Patients with OA would suffer some symptoms, such as stiffness, pain, swelling, and loss of mobility with occasional variable degrees of local inflammation, which would severely reduce the quality of life and create a heavy socioeconomic burden [2]. However, the pathogenesis of OA is not completely understood. Therefore, it is essential to gain novel insights into biological mechanisms of OA and explore potential biomarkers for OA.

With advancement of next-generation sequencing technology, numerous research has increasingly recognized the important role of lncRNAs in the occurrence and development of OA [3]. LncRNAs are RNA

*Correspondence:
Wei Song
songweidr@163.com
Binfei Zhang
zhangbf07@gmail.com
Department of Joint Surgery, Honghui Hospital, Xi'an Jiaotong University, No.555, Youyi East Road Nanshaomen, Xi'an 710054, Shaanxi, China

molecules > 200 bp in length and participate in numerous biological processes, such as the proliferation, apoptosis, cell cycle, and chromatin remodeling [4]. DILC is reduced in OA and over expression of DILC inhibits the expression of IL-6 in chondrocytes [5]. Knockdown of MFI2-AS1 is found to increase cell viability but suppress apoptosis and inflammatory response to inhibit lipopolysaccharide-induced OA progression [6]. MALAT1 is reported to participate in cell proliferation, apoptosis, and ECM degradation of OA [7]. TUG1 performed as a ceRNA through sponging miR-195 to increase MMP-13 expression to regulate ECM degradation in OA [8]. However, the results are not consistent and reliable due to the difference of samples and sequencing platform, which means we need more comprehensive approaches to identify the hub biomarkers.

Therefore, in this study, we analyzed the expression profiles of OA in the Gene Expression Omnibus database (GEO) database by bioinformatics tools to obtain differentially expressed mRNAs (DEmRNAs) and differentially expressed lncRNAs (DElncRNAs). This study aims to better understand the potential mechanisms in the occurrence and development of OA and may accelerate the improvement of the treatment level of OA.

Materials and methods

Microarray data

The mRNA/lncRNA expression profiles of OA were downloaded from GEO database. Three mRNA datasets, GSE113825, GSE117999 and GSE114007, and one lncRNA dataset, GSE113825, were included in this study (Additional file 1: Table S1).

Identification of DEmRNAs/DElncRNAs and functional analysis

With limma package and metaMA package, DEmRNAs and DElncRNAs in OA were obtained. The threshold for the significance was the false discovery rate (FDR) < 0.05. Metascape was employed to perform GO and KEGG pathway enrichment analysis to identify aberrantly regulated biological processes and signaling pathways in OA (p-value < 0.05).

Protein–protein interaction (PPI) network construction

In order to predict the function and explore the mechanism of mRNAs, top 200 up- and down-regulated DEmRNAs were searched with the BioGrid, and PPI network was constructed with Cytoscape software.

Identification of the nearby DEmRNAs of DElncRNAs

To explore the *cis*-regulated mechanism of lncRNAs, the nearby DEmRNAs were identified within a 100 kb window up- or down-stream of DElncRNAs in OA. GO and KEGG pathway enrichment analysis of nearby mRNAs of DElncRNAs was performed by Metascape (p-value < 0.05).

Quantitative reverse transcriptase-polymerase chain reaction (qRT-PCR) validation

Eight blood samples were obtained from 4 patients with OA and 4 normal controls. Samples were collected after obtaining written informed consent from every participant. This study was approved by the ethical committee of Honghui Hospital, Xi'an Jiaotong University Health Science Center (202,112,002) and performed in accordance with the Declaration of Helsinki. Total RNA was isolated with the Trizol reagent (Invitrogen, USA) following manufacturer's protocol. The qRT-PCR reactions were performed in ABI 7300 Real-time PCR Detection System with SuperReal PreMix Plus. GAPDH and ACTB were used as endogenous controls.

Expression validation in the GEO dataset and receiver operating characteristic (ROC) analysis

GSE82107 (involving synovial tissues), GSE55235 (involving synovial tissues), GSE63359 (involving peripheral blood leukocytes), GSE48556 (involving peripheral blood mononuclear cell) and GSE175960 (involving cartilage tissues) datasets were downloaded from the GEO database, which consisted of 175 patients with OA and 79 normal controls. The expression pattern of DEmRNAs and DElncRNAs was validated with these five datasets. Then, by using pROC package in R language, we performed the ROC analysis to assess the diagnostic value of DEmRNAs and DElncRNAs. The area under the curve (AUC) was further calculated.

Results

DEmRNAs and DElncRNAs in OA

After processing the raw data, 2080 (1146 up- and 934 down-regulated) DEmRNAs and 664 (522 up- and 142 down-regulated) DElncRNAs were acquired in OA. The top 10 up- and down-regulated DEmRNAs and DElncRNAs are displayed in Table 1. Hierarchical clustering analysis of DEmRNAs and DElncRNAs is exhibited in Fig. 1A and B, respectively.

Functional analysis of DEmRNAs

GO analysis indicated that axon development (p-value = 1.00E-12), neuron projection morphogenesis (p-value = 1.00E-10) and plasma membrane bounded cell projection morphogenesis (p-value = 1.00E-10)

Table 1 Top 10 up- and down-regulated DEmRNAs/DElncRNAs between patients with OA and normal controls

Symbol	Combined ES	*p*-value	FDR	Regulation
mRNA				
TSPAN11	2.755519	0	0	Up
CFI	2.462673	2.08E-13	7.46E-10	Up
SH3KBP1	2.213482	3.44E-13	1.03E-09	Up
GDE1	1.993256	5.58E-12	7.70E-09	Up
SPOCK1	2.152447	1.81E-11	2.03E-08	Up
SULF1	2.220866	2.67E-11	2.66E-08	Up
TNFAIP6	1.892005	6.03E-11	5.40E-08	Up
HOMER2	1.833474	6.63E-11	5.40E-08	Up
SERPINF1	2.677549	7.89E-11	6.15E-08	Up
AURKA	1.803931	9.32E-11	6.69E-08	Up
MAFF	− 2.94493	0	0	Down
DDIT3	− 2.9291	1.78E-15	1.06E-11	Down
ETS2	− 2.4703	5.91E-14	2.65E-10	Down
MGEA5	− 2.09142	7.62E-13	1.95E-09	Down
CEP95	− 2.0568	2.80E-12	6.27E-09	Down
SLC38A3	− 2.19521	4.12E-12	6.70E-09	Down
FNBP4	− 2.1003	4.49E-12	6.70E-09	Down
STC2	− 2.0997	4.46E-12	6.70E-09	Down
PIM3	− 1.99638	3.73E-12	6.70E-09	Down
PRPF38A	− 1.95241	7.69E-12	9.85E-09	Down
lncRNA				
RP11-754B17.1	0.465715266	1.43E-07	0.001295601	Up
RP1-45I4.3	0.466791971	3.11E-07	0.001295601	Up
RP11-159F24.3	0.246108899	4.63E-07	0.001295601	Up
LINC00412	0.394885033	4.79E-07	0.001295601	Up
RP11-131L23.2	0.467223628	5.71E-07	0.001295601	Up
RP11-293K20.3	0.646913761	5.93E-07	0.001295601	Up
RP11-474P2.7	0.381788287	8.15E-07	0.001556416	Up
RP11-370K11.1	0.301775904	9.39E-07	0.001586651	Up
RP11-381K20.2	0.221602241	1.06E-06	0.001586651	Up
LINC00377	0.235926968	1.32E-06	0.001686864	Up
AC093484.4	− 0.525434637	3.85E-07	0.001295601	Down
RP11-383H13.1	− 0.240895179	1.14E-06	0.001586651	Down
AP001434.2	− 0.50423577	1.72E-06	0.00181637	Down
RP11-212E4.1	− 0.734036745	1.90E-06	0.00181637	Down
RP11-229O3.1	− 0.543410813	3.53E-06	0.002571151	Down
CRNDE	− 0.338423241	4.48E-06	0.002978185	Down
CTB-193M12.5	− 0.307741547	6.89E-06	0.003514563	Down
CTD-2081C10.7	− 0.393448166	6.89E-06	0.003514563	Down
RP11-752L20.3	− 0.464335229	7.16E-06	0.003514563	Down
RP11-244F12.2	− 0.538068417	9.01E-06	0.004050684	Down

DEmRNAs Differentially expressed mRNAs; *DElncRNAs* Differentially expressed lncRNAs; *OA* Osteoarthritis; *ES* Effect size; *FDR* False discovery rate

were significantly enriched GO terms (Fig. 2A). KEGG pathway enrichment analysis showed that PI3K-Akt signaling pathway (p-value = 2.00E-06), endocytosis (p-value = 1.00E-05) and Rap1 signaling pathway (p-value = 5.01E-05) were several significantly enriched pathways (Fig. 2B).

PPI network of DEmRNAs

The PPI network of DEmRNAs contained 135 nodes and 135 edges (Fig. 3). MRNAs with higher degree were as follows: YWHAB (degree = 11), HSPA8 (degree = 8), NEDD4L (degree = 7) and SH3KBP1 (degree = 7).

Identification of the nearby DEmRNAs of DElncRNAs

A total of 46 DElncRNA-nearby DEmRNA pairs, involving 38 DElncRNAs and 45 DEmRNAs, were obtained in OA (Table 2). GO analysis indicated that these DEmRNAs were significantly enriched in protein-DNA complex assembly (p-value = 1.26E-03), protein-DNA complex subunit organization (p-value = 2.00E-03) and head development (p-value = 3.16E-03) (Additional file 2: Fig. S1). In KEGG analysis of nearby DEmRNAs of DElncRNAs, only 3 mRNAs were significantly enriched in the cAMP signaling pathway.

QRT-PCR validation

Seven DEmRNAs (TSPAN11, SULF1, YWHAB, AURKA, SH3KBP1, TRPV2 and ACP5) and two lncRNAs (CRNDE and LINC00152) were selected for qRT-PCR analysis. Based on our integrated analysis, TSPAN11, SULF1, YWHAB, AURKA, SH3KBP1, TRPV2, ACP5 and LINC00152 were up-regulated while CRNDE was down-regulated in OA. Except for CRNDE, the qRT-PCR results were basically in line with our integrated analysis results (Fig. 4).

Expression validation in the GEO dataset and ROC analysis

As shown in Fig. 5, the expression patterns of AURKA, PIK3IP1, SULF1 and TRPV2 in GSE48556, AURKA, B3GALT4, LIMK2, PIK3IP1, SULF1 and TRPV2 in GSE55235, AURKA, B3GALT4, LIMK2, PIK3IP1, SULF1 and TRPV2 in GSE63359, B3GALT4, LIMK2, SULF1, TRPV2, TSPAN11 and CRNDE in GSE82107, B3GALT4, LIMK2, SULF1, TSPAN11, CRNDE and LINC00152 in GSE175960 were displayed, which were consistent with our integrated analysis. We performed ROC curve analyses and calculated the AUC to assess the diagnostic value of these DEmRNAs and DElncRNAs. The results indicated that the AUC of SULF1 (1.000) and TRPV2 (0.900) in GSE55235, and LIMK2 (0.700), SULF1 (0.871) and TSPAN11 (0.829) in GSE82107, was more than 0.70, which indicated that these genes had a potential diagnostic value (Fig. 6).

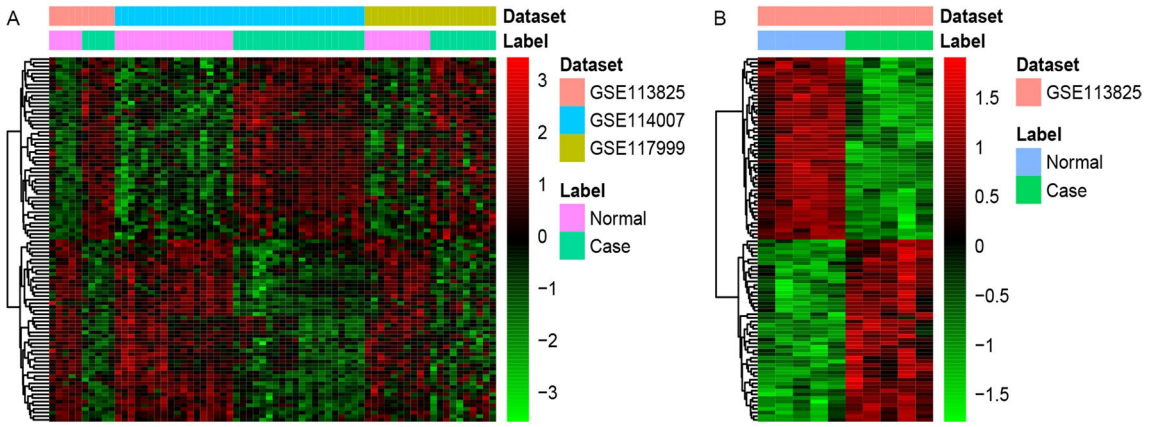

Fig. 1 The heatmap of top 100 up- and down-regulated DEmRNAs (**A**) and DElncRNAs (**B**) in OA

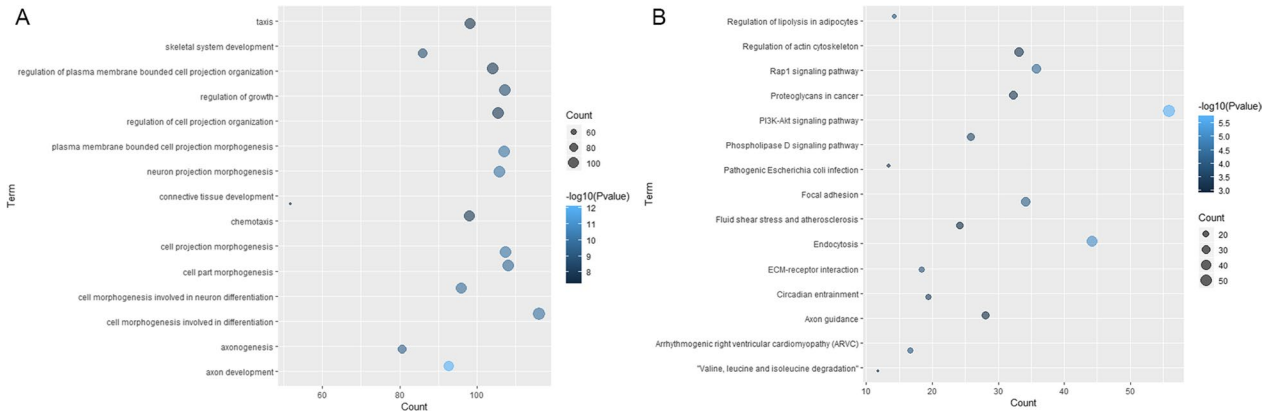

Fig. 2 Significantly enriched GO terms and KEGG pathways of DEmRNAs between OA and normal controls. **A** BP, biological process; **B** KEGG pathways

Discussion

OA is a destructive joint disease, and increases in prevalence with age, marked by disordered cartilage homeostasis with subsequent inflammation and degradation, and seriously threatens human health [9]. Therefore, more attention has been paid on exploring potential pathogenesis mechanisms of OA to facilitate diagnosis and prognosis.

TSPAN11 (CD 151-like) is a member of the tetraspanins family that has been linked to OA. Elevated TSPAN11 is detected in articular cartilage collected from knees undergoing total knee arthroplasty due to end-stage OA [10]. It has been suggested that the integrin clustering mediated by TSPAN11 determines the alignment of bone matrix architecture orthogonal to cell alignment [11]. Human endo-O-sulfatases, including Sulf-1 and Sulf-2, regulate a multitude of cell-signaling events through heparan sulfate protein interactions and have been linked with the occurrence of OA [12]. SULF1 is a regulator of numerous growth factors in skeletal embryonic development [13]. Increased mRNA and protein levels of SULF1 in the cartilage of the elderly patients with OA may alter the sulfation patterns of heparan sulfate proteoglycans and growth factor activities, leading to abnormal chondrocyte activation and cartilage degradation in OA [14]. Jiang et al. indicated that SULF1 was associated with bone loss and the pathology of osteoporosis and OA in aging [15]. The increased expression of Sulf1 in differentiating osteoblasts was further confirmed by RT-PCR analysis of mRNA levels in rat calvarial osteoblast cultures [16]. In this study, both TSPAN11 and SULF1 were significantly high expressed, which was in accordance with previous observations, indicating the importance of TSPAN11 and SULF1 in OA.

As a type of Aurora kinase, Aurora kinase A (AURKA) is crucial for the successful execution of mitosis [17]. Highly expressed AURKA is detected in human osteoarthritic chondrocytes and knocking-down AURKA significantly reduced the OARSI score [18]. AURKA ubiquitination affects mitochondrial dysfunction and

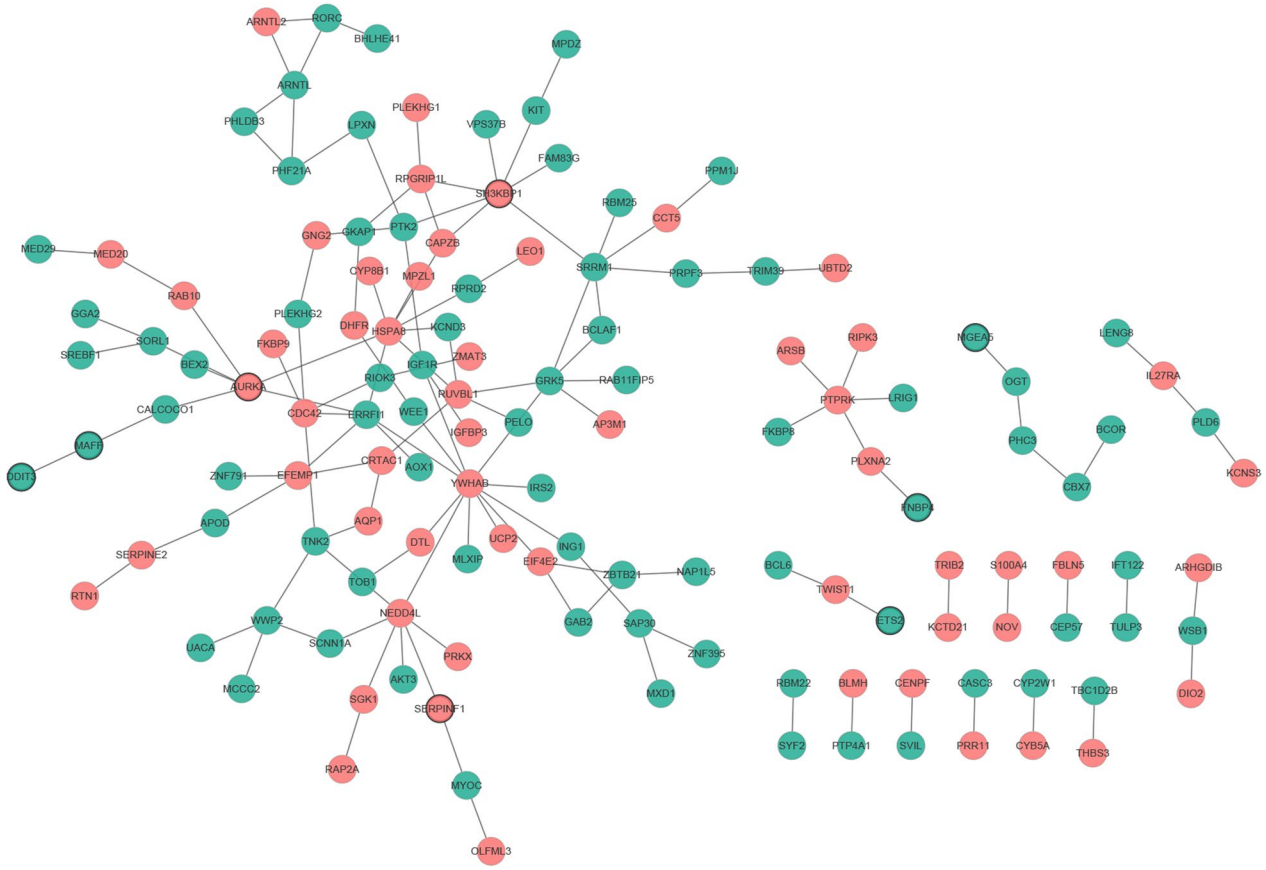

Fig. 3 OA-specific PPI networks

Table 2 Nearby targeted DEmRNAs of DElncRNAs

DElncRNA		Nearby targeted DEmRNA				
Chr	**Symbol**	**Start − 100 kb**	**End + 100 kb**	**Symbol**	**Start**	**End**
6	HCG25	33,149,534	33,354,989	B3GALT4	33,277,132	33,284,832
6	HCG25	33,149,534	33,354,989	WDR46	33,279,108	33,289,527
11	AP000462.1	115,263,629	115,477,931	CADM1	115,169,218	115,504,957
6	SAPCD1-AS1	31,664,310	31,865,588	VWA7	31,765,590	31,777,294
6	SAPCD1-AS1	31,664,310	31,865,588	CLIC1	31,730,581	31,739,763
1	AKT3-IT1	243,693,205	243,894,400	AKT3	243,488,233	243,851,079
6	BVES-AS1	105,036,308	105,269,945	POPDC3	105,158,280	105,179,995
1	AL450992.2	151,741,877	151,950,385	RORC	151,806,071	151,831,872
1	AL450992.2	151,741,877	151,950,385	TDRKH	151,770,107	151,791,416
1	LINC01144	45,203,910	45,405,619	TOE1	45,339,670	45,343,975
15	RAD51-AS1	40,586,243	40,795,107	GCHFR	40,764,020	40,767,710
6	LINC00271	135,397,801	135,816,055	AHI1	135,283,532	135,497,776
17	TMEM220-AS1	10,629,777	10,915,164	ADPRM	10,697,594	10,711,233
4	FAM13A-AS1	88,609,789	88,830,103	NAP1L5	88,695,915	88,697,829
12	RNU7-1	6,843,816	7,043,878	LRRC23	6,873,569	6,914,243
4	SEC24B-AS1	109,247,475	109,533,817	SEC24B	109,433,772	109,540,896
14	ADAM20P1	70,353,541	70,583,775	MED6	70,581,257	70,600,690
10	PRKCQ-AS1	6,480,419	6,716,452	PRKCQ	6,427,143	6,580,301

Table 2 (continued)

DElncRNA		Nearby targeted DEmRNA				
Chr	Symbol	Start − 100 kb	End + 100 kb	Symbol	Start	End
8	EXTL3-AS1	28,596,198	28,801,464	INTS9	28,767,661	28,890,242
21	PAXBP1-AS1	32,628,115	32,843,122	C21orf62	32,793,564	32,813,743
6	RNF217-AS1	124,809,093	125,063,039	RNF217	124,962,545	125,092,633
X	LINC00632	140,609,562	140,893,215	CDR1	140,783,578	140,784,366
22	LINC01521	31,246,777	31,448,719	PIK3IP1	31,281,593	31,292,534
22	LINC01521	31,246,777	31,448,719	LIMK2	31,212,239	31,280,080
1	FOXD2-AS1	47,332,133	47,534,641	FOXD2	47,436,017	47,440,691
4	TAPT1-AS1	16,126,685	16,420,140	TAPT1	16,160,505	16,227,410
6	TRAM2-AS1	52,477,307	52,683,993	EFHC1	52,362,123	52,529,886
3	MCCC1-AS1	182,916,255	183,117,808	MCCC1	183,015,218	183,116,075
18	NDUFV2-AS1	9,021,265	9,236,645	ANKRD12	9,136,228	9,285,985
16	SSTR5-AS1	964,093	1,178,731	SSTR5	1,078,781	1,080,142
16	SSTR5-AS1	964,093	1,178,731	CACNA1H	1,153,121	1,221,772
2	AC012506.4	23,275,229	23,481,299	KLHL29	23,385,217	23,708,611
12	RERG-IT1	15,012,363	15,214,698	RERG	15,107,783	15,348,675
15	SNHG21	82,650,564	82,857,206	WHAMM	82,809,628	82,836,108
15	SNHG21	82,650,564	82,857,206	HOMER2	82,836,946	82,986,153
11	AP001372.2	74,393,366	74,598,533	PGM2L1	74,330,318	74,398,473
11	AP001372.2	74,393,366	74,598,533	KCNE3	74,454,841	74,467,729
17	SOX9-AS1	71,934,107	72,337,203	SOX9	72,121,020	72,126,420
21	C21orf62-AS1	32,672,100	32,993,735	C21orf62	32,793,564	32,813,743
14	DICER1-AS1	95,057,645	95,279,933	CLMN	95,181,940	95,319,906
9	RMRP	35,557,751	35,758,018	CD72	35,609,533	35,646,810
17	AC093484.4	16,340,479	16,540,952	CENPV	16,342,534	16,353,656
17	AC093484.4	16,340,479	16,540,952	TRPV2	16,415,542	16,437,003
3	TMEM44-AS1	194,484,011	194,690,260	FAM43A	194,686,544	194,689,037
7	LINC00174	66,276,044	66,593,566	TPST1	66,205,199	66,420,543
10	SFTA1P	10,684,437	10,894,980	CELF2	10,798,397	11,336,675

DEmRNAs Differentially expressed mRNAs; *DElncRNAs* Differentially expressed lncRNAs

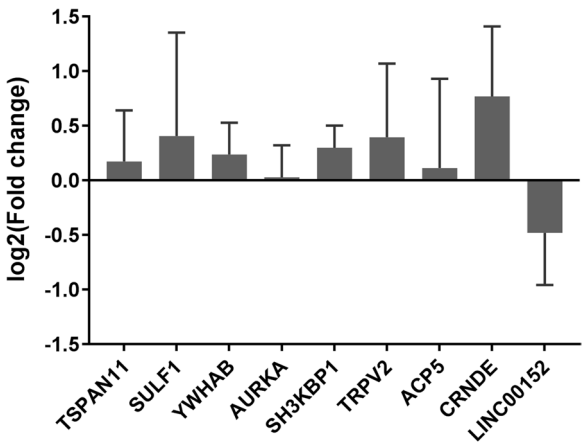

Fig. 4 QRT-PCR results of the DEmRNAs and DElncRNAs in OA

inhibits the occurrence of OA by degradation of SOD2 [19]. AURKA is identified as a hub gene in osteoarthritic degenerative meniscal lesions based on GSE52042 dataset [20]. Similarly, we found that AURKA was identified not only as a significantly up-regulated DEmRNA, but also as a hub gene in this study, which added to evidence that AURKA is crucial for the development of OA.

CRNDE is closely associated with the proliferation of osteoclasts [21]. CRNDE regulates bone marrow mesenchymal stem cells chondrogenic differentiation to promote cartilage repair in OA [22]. CRNDE is a regulator of bone metabolism, and deletion of CRNDE in mice develops a low bone mass phenotype due to impaired bone formation [23]. Overexpression of CRNDE alleviated cartilage damage and synovitis in OA rats [24]. Wang et al.

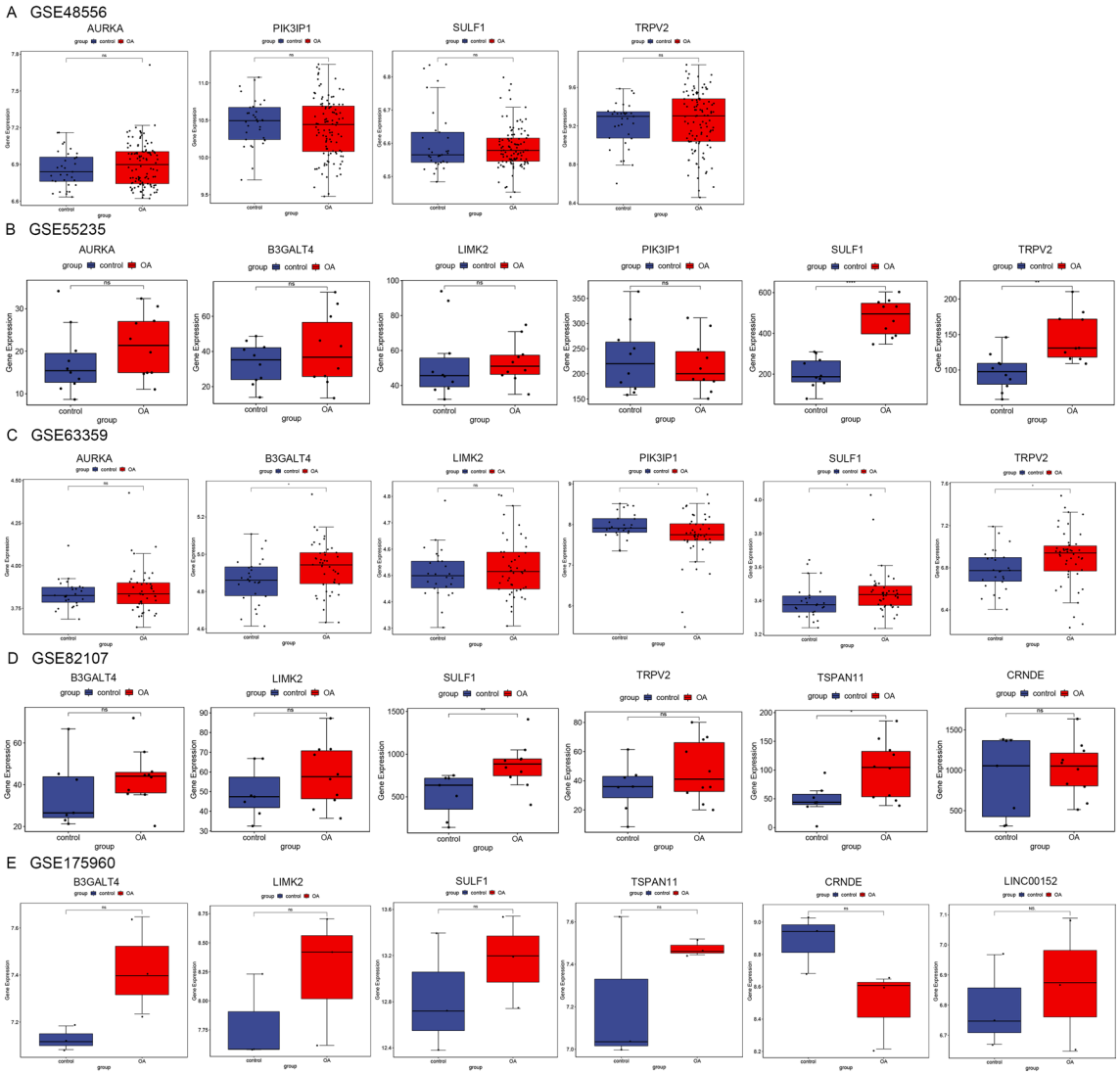

Fig. 5 Expression validations of DEmRNAs and DElncRNAs in GSE48556 (**A**), GSE55235 (**B**), GSE63359 (**C**), GSE82107 (**D**) and GSE175960 (**E**) databases. The x-axis shows control and OA and the y-axis shows expression levels

demonstrated that LINC00152 induced proliferation and suppressed apoptosis in rheumatoid arthritis fibroblast-like synoviocytes [25]. Similarly, Zhang et al. suggested that LINC00152 was inflammation-related lncRNA and might be involved in the regulation of rheumatoid arthritis fibroblast-like synoviocytes inflammation [26]. In addition, Hu et al. identified that CRNDE and LINC00152 were involved in age-related degeneration of articular cartilage [27]. In agreement with previous studies, we also observed significantly down-regulated CRNDE and LINC00152 in this study.

LIM kinases (LIMKs), comprising LIMK1 and LIMK2, are common downstream effectors of several signalization pathways, and function as a signalling node that controls cytoskeleton dynamics through the phosphorylation of the cofilin family proteins [28]. Li et al. suggested that LIMK2 is required for membrane cytoskeleton reorganization of contracting airway smooth muscle [29]. LIMK2 plays an important role in the reorganization of actin cytoskeleton induced by fluid shear stress in murine osteoblast lines [30]. LIMK2 silencing inhibits the fluid shear stress-induced reorganisation of the actin cytoskeleton of primary osteoblasts and demonstrates that the mechanosensitivity of osteoblasts in response to this stress is enhanced [31]. PIK3IP1 is reported as a negative regulator of the PI3K pathway [32]. PIK3IP1 has also been considered as a negative regulator of anti-tumor T cell response [33]. PIK3IP1 is an important

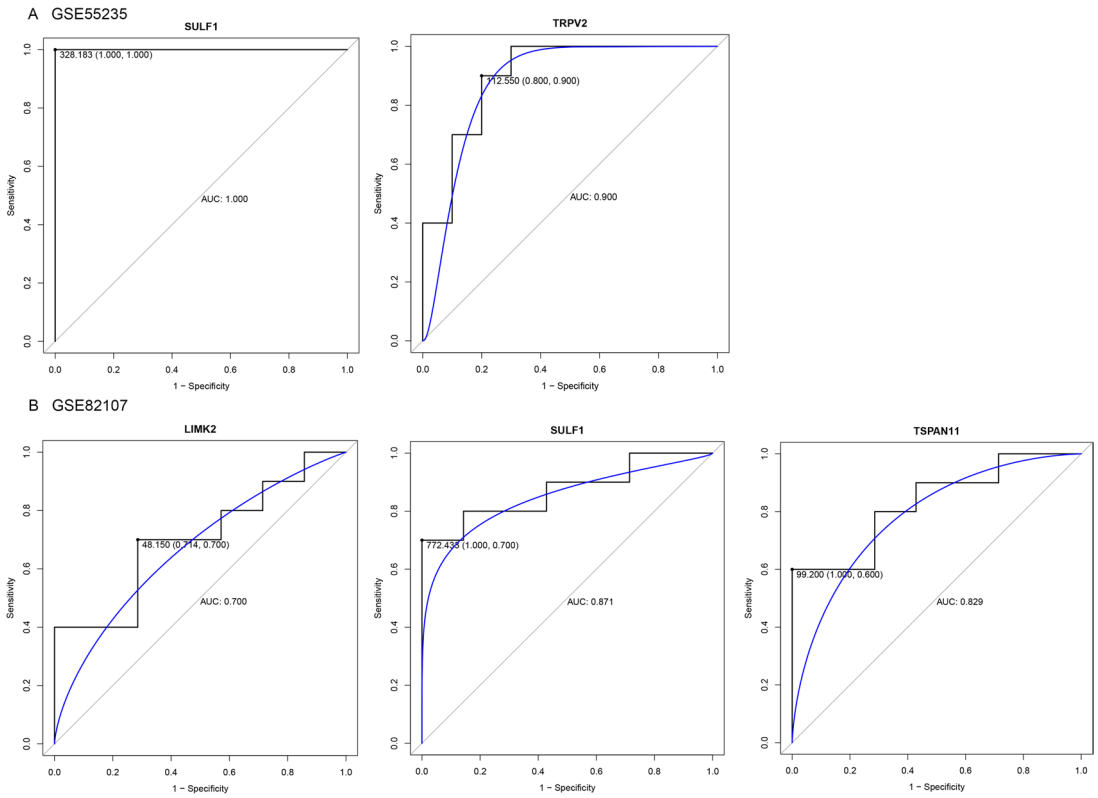

Fig. 6 The ROC curves of DEmRNAs and DElncRNAs in GSE55235 (**A**) and GSE82107 (**B**) databases. The x-axes show 1-specificity (the proportion of false positives) and y-axes show sensitivity (the proportion of true positives)

modulator for the tumor necrosis factor-driven inflammatory response in fibroblast-like synoviocytes [34]. In addition, down-regulated PIK3IP1 is detected in rheumatoid arthritis [35]. Both LIMK2 and PIK3IP1 interacted with LINC00152, which indicated that the LINC00152/LIMK2 and LINC00152/PIK3IP1 interacted pairs may exert a critical function in OA.

TRPV2 encodes an ion channel which is a Ca^{2+} permeable channel and performs a function in mediating intracellular Ca^{2+} current via mechanical stimuli [36]. Bai et al. reported that TRPV2 modulated RANKL-dependent osteoclastic differentiation in multiple myeloma cells [37]. Laragione et al. indicated that TRPV2 inhibited cell invasion, inflammatory cell infiltration, and angiogenesis, and reduced the severity of arthritis [38]. TRPV2 is required for homeostasis of articular joints by induction of Prg4 and suppression of ectopic endochondral ossification in these joints [36]. In the present study, significantly up-regulated TRPV2 was detected in OA, which may suggest that TRPV2 is of great importance in OA. In addition, AC093484.4, as the most significant DElncRNA, interacted with TRPV2. Hence, more evidence should be obtained to determine the function of AC093484.4/TRPV2 interact pair on OA.

The β-1,3-galactosyltransferase-4 (B3GALT4) gene belongs to the β-1,3-galactosyltransferase (β3GalT) gene family, which is essential in the O-glycosylation process [39]. B3GALT4 has been linked to multiple tumors. For example, B3GALT4 is suggested to serve as a novel biomarker for the diagnosis of gynecological cancers [40]. Zhang et al. revealed that B3GALT4 was a novel prognostic biomarker for colorectal cancer [41]. Zhang et al. reported that higher expression levels of B3GALT4 predicted better overall survival rates, which might be potential predictors of recurrent osteosarcoma prognosis [42]. In addition, Verma et al. indicated that decreased B3GALT4 could increase cell vulnerability to potentially toxic stressors, which may contribute to dopaminergic neurodegeneration in Parkinson's disease [43]. Shi et al. indicated that HCG25 was significantly up-regulated in hepatocellular carcinoma and had great diagnostic value for hepatocellular carcinoma [44]. To date, there is no study report on the association between OA and HCG25/B3GALT4. In this study, B3GALT4 was interacted with HCG25, which remind us to focus on the function of HCG25/B3GALT4 interact pair on OA.

Our study also has certain limitations. First, the data for this study was obtained from public databases with a

small sample size. However, the external validation database confirmed the reliability of our analysis. Second, the sample size used for QRT-PCR validation was small. Third, molecular experiments as well as larger clinical samples are required to further validate the results.

Conclusion

In conclusion, we identified several DEmRNAs and DElncRNAs associated with OA. This study thus provides further insights into the underlying molecular mechanism of OA, which may facilitate the diagnosis and treatment of OA.

Abbreviations

OA	Osteoarthritis
GEO	Gene expression omnibus database
DEmRNAs	Differentially expressed mRNAs
DElncRNAs	Differentially expressed lncRNAs
PPI	Protein–protein interaction
qRT-PCR	Quantitative reverse transcriptase-polymerase chain reaction
ROC	Receiver operating characteristic
AUC	Area under the curve
AURKA	Aurora kinase A
LIMKs	LIM kinases
B3GALT4	β-1,3-galactosyltransferase-4
β3GalT	β-1,3-galactosyltransferase
FDR	False discovery rate

Supplementary Information

The online version contains supplementary material available at https://doi.org/10.1186/s42358-023-00288-1.

Additional file 1: Table S1. List of mRNA/lncRNA study samples from GEO database.

Additional file 2: Fig. S1. Biological processes related to nearby DEmRNAs of DElncRNAs in OA.

Acknowledgements

Not applicable.

Author contributions

JW and WS contributed to the study conception and design. Material preparation, data collection and analysis were performed by JW, YZ, TM, BZ, FX, PW and HC. The first draft of the manuscript was written by JW, and all authors commented on previous versions of the manuscript. All authors read and approved the final manuscript.

Funding

This research did not receive any specific Grant from funding agencies in the public, commercial, or not-for-profit sectors.

Availability of data and materials

All data generated or analysed during this study are included in this published article.

Declarations

Ethics approval and consent to participate

This study was approved by the ethical committee of Honghui Hospital, Xi'an Jiaotong University (202112002). All participants were informed as to the purpose of this study, and that this study complied with the Declaration of Helsinki. The written consent was obtained from the all patients.

Consent for publication

The subjects gave written informed consent for the publication of any associated data and accompanying images.

Competing interests

The authors declare that they have no competing interests.

Received: 13 July 2022 Accepted: 18 February 2023
Published online: 27 February 2023

References

1. Mathiessen A, Conaghan PG. Synovitis in osteoarthritis: current understanding with therapeutic implications. Arthritis Res Ther. 2017;19:18.
2. Glyn-Jones S, Palmer AJ, Agricola R, Price AJ, Vincent TL, Weinans H, et al. Osteoarthritis. Lancet. 2015;386:376–87.
3. Xie F, Liu YL, Chen XY, Li Q, Zhong J, Dai BY, et al. Role of MicroRNA, LncRNA, and exosomes in the progression of osteoarthritis: a review of recent literature. Orthop Surg. 2020;12:708–16.
4. Ma L, Bajic VB, Zhang Z. On the classification of long non-coding RNAs. RNA Biol. 2013;10:925–33.
5. Huang J, Liu L, Yang J, Ding J, Xu X. lncRNA DILC is downregulated in osteoarthritis and regulates IL-6 expression in chondrocytes. J Cell Biochem. 2019;120:16019–24.
6. Luo X, Wang J, Wei X, Wang S, Wang A. Knockdown of lncRNA MFI2-AS1 inhibits lipopolysaccharide-induced osteoarthritis progression by miR-130a-3p/TCF4. Life Sci. 2020;240: 117019.
7. Zhang Y, Wang F, Chen G, He R, Yang L. LncRNA MALAT1 promotes osteoarthritis by modulating miR-150-5p/AKT3 axis. Cell Biosci. 2019;9:54.
8. Tang LP, Ding JB, Liu ZH, Zhou GJ. LncRNA TUG1 promotes osteoarthritis-induced degradation of chondrocyte extracellular matrix via miR-195/MMP-13 axis. Eur Rev Med Pharmacol Sci. 2018;22:8574–81.
9. Zhang X, Bu Y, Zhu B, Zhao Q, Lv Z, Li B, et al. Global transcriptome analysis to identify critical genes involved in the pathology of osteoarthritis. Bone Jt Res. 2018;7:298–307.
10. Rai MF, Tycksen ED, Cai L, Yu J, Wright RW, Brophy RH. Distinct degenerative phenotype of articular cartilage from knees with meniscus tear compared to knees with osteoarthritis. Osteoarthr Cartil. 2019;27:945–55.
11. Nakanishi Y, Matsugaki A, Kawahara K, Ninomiya T, Sawada H, Nakano T. Unique arrangement of bone matrix orthogonal to osteoblast alignment controlled by Tspan11-mediated focal adhesion assembly. Biomaterials. 2019;209:103–10.
12. Chiu LT, Sabbavarapu NM, Lin WC, Fan CY, Wu CC, Cheng TR, et al. Trisaccharide sulfate and its sulfonamide as an effective substrate and inhibitor of human endo-O-sulfatase-1. J Am Chem Soc. 2020;142:5282–92.
13. Isidor B, Pichon O, Redon R, Day-Salvatore D, Hamel A, Siwicka KA, et al. Mesomelia-synostoses syndrome results from deletion of SULF1 and SLCO5A1 genes at 8q13. Am J Hum Genet. 2010;87:95–100.
14. Otsuki S, Taniguchi N, Grogan SP, D'Lima D, Kinoshita M, Lotz M. Expression of novel extracellular sulfatases Sulf-1 and Sulf-2 in normal and osteoarthritic articular cartilage. Arthritis Res Ther. 2008;10:R61.
15. Jiang SS, Chen CH, Tseng KY, Tsai FY, Wang MJ, Chang IS, et al. Gene expression profiling suggests a pathological role of human bone marrow-derived mesenchymal stem cells in aging-related skeletal diseases. Aging (Albany NY). 2011;3:672–84.
16. Zaman G, Staines KA, Farquharson C, Newton PT, Dudhia J, Chenu C, et al. Expression of Sulf1 and Sulf2 in cartilage, bone and endochondral fracture healing. Histochem Cell Biol. 2016;145:67–79.
17. Bertolin G, Tramier M. Insights into the non-mitotic functions of Aurora kinase A: more than just cell division. Cell Mol Life Sci. 2020;77:1031–47.
18. Yang Q, Zhou Y, Cai P, Fu W, Wang J, Wei Q, et al. Up-regulated HIF-2α contributes to the osteoarthritis development through mediating the primary cilia loss. Int Immunopharmacol. 2019;75: 105762.

19. Yang C, You D, Huang J, Yang B, Huang X, Ni J. Effects of AURKA-mediated degradation of SOD2 on mitochondrial dysfunction and cartilage homeostasis in osteoarthritis. J Cell Physiol. 2019;234:17727–38.
20. Huan X, Jinhe Y, Rongzong Z. Identification of pivotal genes and pathways in osteoarthritic degenerative meniscal lesions via bioinformatics analysis of the GSE52042 dataset. Med Sci Monit. 2019;25:8891–904.
21. Li W, Zhu HM, Xu HD, Zhang B, Huang SM. CRNDE impacts the proliferation of osteoclast by estrogen deficiency in postmenopausal osteoporosis. Eur Rev Med Pharmacol Sci. 2018;22:5815–21.
22. Shi C, Zheng W, Wang J. lncRNA-CRNDE regulates BMSC chondrogenic differentiation and promotes cartilage repair in osteoarthritis through SIRT1/SOX9. Mol Cell Biochem. 2021;476:1881–90.
23. Mulati M, Kobayashi Y, Takahashi A, Numata H, Saito M, Hiraoka Y, et al. The long noncoding RNA Crnde regulates osteoblast proliferation through the Wnt/β-catenin signaling pathway in mice. Bone. 2020;130: 115076.
24. Zhang Z, Yang P, Wang C, Tian R. LncRNA CRNDE hinders the progression of osteoarthritis by epigenetic regulation of DACT1. Cell Mol Life Sci. 2022;79:405.
25. Wang W, Guo P, Chen M, Chen D, Cheng Y, He L. FOXM1/LINC00152 feedback loop regulates proliferation and apoptosis in rheumatoid arthritis fibroblast-like synoviocytes via Wnt/β-catenin signaling pathway. Biosci Rep. 2020;40(1):BSR20191900. https://doi.org/10.1042/BSR20191900.
26. Zhang J, Gao FF, Xie J. LncRNA linc00152/NF-κB feedback loop promotes fibroblast-like synovial cells inflammation in rheumatoid arthritis via regulating miR-103a/TAK1 axis and YY1 expression. Immun Inflamm Dis. 2021;9:681–93.
27. Hu P, Sun F, Ran J, Wu L. Identify CRNDE and LINC00152 as the key lncRNAs in age-related degeneration of articular cartilage through comprehensive and integrative analysis. PeerJ. 2019;7: e7024.
28. Brion R, Regnier L, Mullard M, Amiaud J, Rédini F, Verrecchia F. LIM kinases in osteosarcoma development. Cells. 2021;10:3542.
29. Li Y, Zhou Y, Wang P, Tao T, Wei L, Wang Y, et al. LIMK2 is required for membrane cytoskeleton reorganization of contracting airway smooth muscle. J Genet Genomics. 2021;48:452–62.
30. Fu Q, Wu C, Shen Y, Zheng S, Chen R. Effect of LIMK2 RNAi on reorganization of the actin cytoskeleton in osteoblasts induced by fluid shear stress. J Biomech. 2008;41:3225–8.
31. Yang Z, Tan S, Shen Y, Chen R, Wu C, Xu Y, et al. Inhibition of FSS-induced actin cytoskeleton reorganization by silencing LIMK2 gene increases the mechanosensitivity of primary osteoblasts. Bone. 2015;74:182–90.
32. Fruman DA, Chiu H, Hopkins BD, Bagrodia S, Cantley LC, Abraham RT. The PI3K pathway in human disease. Cell. 2017;170:605–35.
33. Chen Y, Wang J, Wang X, Li X, Song J, Fang J, et al. Pik3ip1 is a negative immune regulator that inhibits antitumor T-cell immunity. Clin Cancer Res. 2019;25:6180–94.
34. Brandstetter B, Dalwigk K, Platzer A, Niederreiter B, Kartnig F, Fischer A, et al. FOXO3 is involved in the tumor necrosis factor-driven inflammatory response in fibroblast-like synoviocytes. Lab Invest. 2019;99:648–58.
35. Badr MT, Häcker G. Gene expression profiling meta-analysis reveals novel gene signatures and pathways shared between tuberculosis and rheumatoid arthritis. PLoS ONE. 2019;14: e0213470.
36. Nakamoto H, Katanosaka Y, Chijimatsu R, Mori D, Xuan F, Yano F, et al. Involvement of transient receptor potential vanilloid channel 2 in the induction of lubricin and suppression of ectopic endochondral ossification in mouse articular cartilage. Arthritis Rheumatol. 2021;73:1441–50.
37. Bai H, Zhu H, Yan Q, Shen X, Lu X, Wang J, et al. TRPV2-induced Ca(2+)-calcineurin-NFAT signaling regulates differentiation of osteoclast in multiple myeloma. Cell Commun Signal. 2018;16:68.
38. Laragione T, Cheng KF, Tanner MR, He M, Beeton C, Al-Abed Y, et al. The cation channel Trpv2 is a new suppressor of arthritis severity, joint damage, and synovial fibroblast invasion. Clin Immunol. 2015;158:183–92.
39. Wandall HH, Blixt O, Tarp MA, Pedersen JW, Bennett EP, Mandel U, et al. Cancer biomarkers defined by autoantibody signatures to aberrant O-glycopeptide epitopes. Cancer Res. 2010;70:1306–13.
40. Seko A, Kataoka F, Aoki D, Sakamoto M, Nakamura T, Hatae M, et al. Beta 1,3-galactosyltransferases-4/5 are novel tumor markers for gynecological cancers. Tumour Biol. 2009;30:43–50.
41. Zhang T, Wang F, Wu JY, Qiu ZC, Wang Y, Liu F, et al. Clinical correlation of B7–H3 and B3GALT4 with the prognosis of colorectal cancer. World J Gastroenterol. 2018;24:3538–46.
42. Zhang M, Liu Y, Kong D. Identifying biomolecules and constructing a prognostic risk prediction model for recurrence in osteosarcoma. J Bone Oncol. 2021;26: 100331.
43. Verma M, Schneider JS. siRNA-mediated knockdown of B3GALT4 decreases GM1 ganglioside expression and enhances vulnerability for neurodegeneration. Mol Cell Neurosci. 2019;95:25–30.
44. Shi B, Zhang X, Chao L, Zheng Y, Tan Y, Wang L, et al. Comprehensive analysis of key genes, microRNAs and long non-coding RNAs in hepatocellular carcinoma. FEBS Open Bio. 2018;8:1424–36.

Publisher's Note